Coupling the Multi Phase-Field Method with an Electro-Thermal Solver to Simulate Phase Change Mechanisms in Ge-rich GST based PCM

Raphaël Bayle
STMicroelectronics
Ecole Polytechnique, CNRS, IP Paris
CEA, LETI, Univ. Grenoble Alpes

Olga Cueto
CEA, LETI, Univ. Grenoble Alpes
Grenoble, France
olga.cueto@cea.fr

Serge Blonkowski
CEA, LETI, Univ. Grenoble Alpes
Grenoble, France

Thomas Philippe
Lab. Physique de la Matière Condensée
Ecole Polytechnique, CNRS, IP Paris
Palaiseau, France

Hervé Henry
Lab. Physique de la Matière Condensée
Ecole Polytechnique, CNRS, IP Paris
Palaiseau, France

Mathis Plapp
Lab. Physique de la Matière Condensée
Ecole Polytechnique, CNRS, IP Paris
Palaiseau, France

***Abstract*—The ternary alloy GeSbTe is widely used as material for phase-change memories. Thanks to an optimized Ge-rich GeSbTe alloy, the crystallizion temperature of the alloy is increased and the stability requirements of high working temperature required for automotive applications are fullfilled, but the crystallization of the Ge-rich alloy proceeds with a composition change and a phase separation. We have developed a multi-phase-field model for the crystallization of the Ge-rich GeSbTe alloy and we have coupled it to an electro-thermal solver. This model is able to capture both the emergence of a two-phase polycristalline structure starting from an initially amorphous material, and the melting and recrystallization during the device operations.**

***Index Terms*—Phase Change Memories, simulation, crystallization with segregation, multi phase-field method**

I. Introduction

This work is part of the development of the co-integration of 28nm Fully Depleted Silicon on Insulator (FD-SOI) advanced CMOS technology with an electrical non volatile Phase Change Memory (PCM) based on a chalcogenide ternary material for automotive micro-controller applications [1]. Thanks to an optimized Ge-rich GeSbTe alloy, a good trade-off between set speed and data retention performances is obtained [2]. In particular, the crystallization temperature of the Ge-rich GeSbTe (Ge-rich GST) alloy can be raised up to 200°C in comparison with that of the stoichiometric alloy $Ge_2Sb_2Te_5$ (GST). This helps to fulfill the stability requirements of high working temperature required for automotive applications. The Ge-rich alloy does not crystallize congruently: the crystallization proceeds with a composition change and a phase separation. The additional Ge is rejected into the amorphous phase upon crystallization of GST, which leads to the nucleation and growth of an additional crystalline phase that is almost pure Ge. Since Ge and GST phase have strongly different physical properties, it is of critical importance to understand the crystallization process of Ge-rich GST. The Multi Phase-Field Method (MPFM) is an extension of the Phase-Field Method (PFM) widely used for alloys with non congruent crystallization. Phase Field Models are continuum models based on non equilibrium thermodynamics used in materials science to simulate the evolution of microstructures in a wide variety of processes. In a previous work, we had implemented the PFM for the congruent GST alloy [3]. Here, we present a new implementation of the MPFM for the Ge-rich GST alloy and its coupling with a finite element electro-thermal solver.

II. MPFM with Orientation Fields

We assume that our alloy can be described in a quasibinary approximation: instead of considering that the concentration of Sb, Te and Ge are independent, we assume that the three concentrations evolve on a predetermined segment of the ternary diagram Sb-Te-Ge. The chosen segment links stoichiometric GST to pure Ge and we use as a reference the pseudobinary phase diagram along a line reaching from Sb_2Te_3 to pure Ge given in [8] which is close to the segment we consider. The parameter c in the model accounts for the position on this segment: $c = 0$ corresponds to stoichiometric phase (GST) and $c = 1$ to quasi-pure Ge phase (Ge). Three phases are considered: the crystalline GST, the crystalline Ge, and the disordered phase (amorphous/melted). The model relies on three phase fields p_i, $i = 1, 2, 3$, that correspond to the local volume fractions of the three phases and thus satisfy $p_i \in [0, 1] \, \forall i$ and $\sum_i p_i = 1$.

In addition, our model takes into account the orientations of the crystalline grains through two fields θ_1 and θ_2 encoding the orientation in phase Ge and GST. This adds complexity to the model and can lead to numerical singularities. Despite increased complexity, taking into account the grain orientation allows to track grain boundaries and to follow their evolution. This helps to understand the role of grain boundaries in the

complex electrical behaviour of GST alloys (e.g. drift of the Set state).

Following the insight that the appropriate thermodynamical potential for systems with exchanges of matter is the grand-potential rather than the free-energy [5] [6], a grand-potential functional is used:

$$\Omega = \int_V \omega \, dV, \tag{1}$$

defined as the volume integral of a grand-potential density.

$$\omega(\mathbf{p}, \vec{\nabla}\mathbf{p}, \mu, T) = K\omega_{\text{grad}}(\vec{\nabla}\mathbf{p}) + H\omega_p(\mathbf{p}) + \omega_{\text{th}}(\mathbf{p}, \mu, T) \tag{2}$$

where μ is the chemical potential defined by $\mu = \partial f/\partial c$, T is the temperature and $\mathbf{p}$ is the vector (p_1,p_2,p_3).

$$\omega_{\text{grad}} = \frac{1}{2}\sum_i \left(\vec{\nabla p_i}\right)^2, \tag{3}$$

ω_{grad} sets a free-energy cost for gradients in p, forcing interfaces to have a finite width, and K has dimensions of energy per unit length.

$$\omega_p = \omega_{\text{TW}} = \sum_i p_i^2(1-p_i)^2. \tag{4}$$

ω_p depends only on the phase fields and provides an "energy landscape" in $\mathbf{p}$ and H is a constant with dimensions of energy per unit volume.

ω_{th} is the thermodynamic part of the grand-potential

$$\omega_{th}(\mu, T) = \sum_i g_i(\mathbf{p})\omega_i(\mu, T), \tag{5}$$

where the ω_i are given by (6) and the $g_i(p_i, p_j, p_k)$ are interpolation functions taken as proposed by [5].

The grand-potential ω is defined as the Legendre transform of the free-energy f, that is,

$$\omega_i(\mu, T) = f_i(c, T) - \mu c_i(\mu, T) \tag{6}$$

where $c_i(\mu, T)$ is the inverse of $\mu_i(c, T) = \partial f_i/\partial c$. The invertibility of the μ_i functions is required here; this condition is equivalent to the convexity of free energy functions at any temperature.

The p_i, i=1,2 are assumed to evolve towards the minimum of Ω,

$$\frac{\partial p_i}{\partial t} = -\Gamma \left.\frac{\delta\Omega}{\delta p_i}\right|_{p_1+p_2+p_3=1}, \text{ i=1,2} \tag{7}$$

where Γ is a relaxation rate constant.

The interface width W and the relaxation time τ are defined by

$$W = \sqrt{\frac{K}{H}}, \tag{8}$$

$$\tau = \frac{1}{\Gamma H} \tag{9}$$

An implementation of the orientation model was chosen taking benefit of the model proposed in [4] for a single cristalline phase case. A coupling term is added to (7):

$$\frac{\partial p_i}{\partial t} = -\Gamma \left.\frac{\delta\Omega}{\delta p_i}\right|_{p_1+p_2+p_3=1} - \Gamma C_\theta q'(p_i)(\vec{\nabla}\theta_i)^2, \text{ i=1,2} \tag{10}$$

where C_θ is a constant associated to the energy of the grain boundaries. This coupling term is chosen in order to restore the model proposed in [4] when one of the 2 cristallines phases is missing. The function q is the coupling function introduced in [4]:

$$q(p_i) = \frac{7p_i^3 - 6p_i^4}{(1-p_i)^3}. \tag{11}$$

Finally, the non-conserved phase-fields evolve as:

$$\begin{aligned}\tau\frac{\partial p_i}{dt} &= W^2\nabla^2 p_i + \frac{2}{3}F_{\text{TW}}(p_i) \\ &\quad -\frac{1}{H}\sum_j \omega_i(\mu)\frac{\partial g_j}{\partial p_i}\Big|_{\sum_i p_i=1} \\ &\quad -\frac{C_\theta}{H}q'(p_i)(\vec{\nabla}\theta_i)^2, \text{ i=1,2}\end{aligned} \tag{12}$$

with $F_{\text{TW}}(p_i) = -2p_i(1-p_i) + \sum_{j\neq i} p_j(1-p_j)(1-2p_j)$

The orientation fields evolve as:

$$\tau_{\theta_i}\partial_t\theta_i = \frac{1}{q(p_i)}\nabla.(q(p_i)\vec{\nabla}\theta_i), \text{ i=1,2} \tag{13}$$

where τ_{θ_i} are relaxation times for the orientation fields.

The concentration c is a conserved field, and thus obeys the continuity equation

$$\frac{\partial c}{\partial t} + \nabla \cdot \vec{J} = 0, \tag{14}$$

where the flux $\vec{J}$ is driven by the gradient of the diffusion potential

$$\vec{J} = -M(\mu, p)\vec{\nabla}\mu \tag{15}$$

with $M(\mu, p)$ the mobility of Ge. In order to ensure the conservation of matter with the best numerical accuracy, the chemical diffusion (14) is solved using c as a variable rather than μ. Due to the convexity of the free-energies, μ can be easily calculated from c by inversion of $c = \sum_i g_i(p)c_i(\mu, T)$.

III. Thermodynamic and material model

The PFM requires the choice of a free energy for each phase as a function of the concentration and temperature. Our energy model has been obtained by assuming a regular solution model and by merging two lens-shape phase diagrams to get an eutectic phase diagram with reasonable value for the eutectic composition and temperature (Fig. 1).

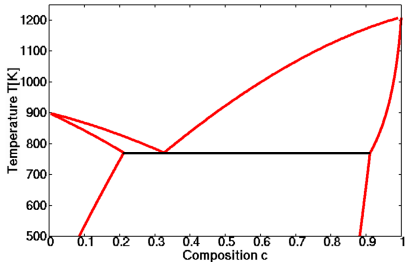

Fig. 1: Phase diagram obtained from the free energy functions

Among the parameters to be fixed, the constants H and K are related to the interface width W by (8) and to the

interface free energy σ by $\sigma = \sqrt{2KH}/3$ [5]. The parameter interface width is chosen to be $W = 5\ 10^{-10}m$, which is a physically realistic value for solid-liquid interfaces. The value $\sigma = 0.4J/m^2$ is extracted for the surface energy near 700K from data about surface tension for amorphous-crystalline interfaces in germanium [10].
The relaxation time τ is evaluated from kinetic data for GST225 [7] and the relaxation times for orientation fields τ_{θ_i} are deduced from τ.
$M(\mu, p)$, the mobility of Ge, is used to evaluate the diffusion flux of the equation (15). It is evaluated from $D(\mu, p)$, the diffusivity of Ge, using the relation $M(\mu, p) = D(\mu, p)\partial c/\partial\mu$. Diffusivity of Ge has been chosen for both the crystalline phases and the amorphous phases according to the one used in GST225 [9]. Near 700K, Ge diffusivity is found to be close to $10^{-9}m^2/s$ in the amorphous and close to $10^{-12}m^2/s$ in the crystalline phases.

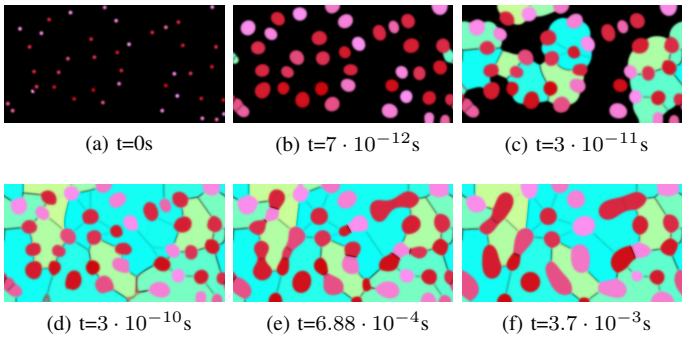

(a) t=0s (b) t=$7 \cdot 10^{-12}$s (c) t=$3 \cdot 10^{-11}$s

(d) t=$3 \cdot 10^{-10}$s (e) t=$6.88 \cdot 10^{-4}$s (f) t=$3.7 \cdot 10^{-3}$s

Fig. 2: Temporal evolution of the crystalline state in 2D simulation of the crystallization of an amorphous layer of Ge-rich GST. Amorphous areas are represented in black. The different shades of pink/red stand for crystalline Ge phase and green/blue for GST phase.

IV. Crystallization of an amorphous layer

In the production of PCM devices, the PCM material is deposited amorphous, but crystallizes during subsequent heat treatments. In order to model the initial state of the material before operations of the device, we must therefore simulate the crystallization of an amorphous layer. Accordingly, the MPFM model is used to simulate an isothermal crystallization at 673K during 3.7ms. The simulation domain is 150 nm wide and 100 nm high. A nucleation scenario inferred from experimental observations is used [11]. During the annealing of an amorphous layer of Ge-rich GST, it is observed that the Ge crystallizes first, followed by nucleation of the GST phase, for temperature above 673K. Thus in the simulation, grains of the Ge phase are introduced initially randomly in the amorphous matrix (Fig. 2a). Their subsequent growth drains Ge from the matrix. When the latter is sufficiently impoverished in Ge, the GST phase can nucleate. The GST nuclei are randomly introduced as soon as a critical concentration of 0.35 is reached locally. After many nucleation events and some growth of the nuclei, grain boundaries are formed between the GST grains (Fig. 2c). Even when the crystallization has completed (Fig. 2d), the microstructures are still evolving (Fig. 2e and Fig. 2f). This reorganization occurs mainly by two ways. The first one is the Ostwald ripening: small grains dissolve while bigger ones grow. Since Ge grains pin the grain boundaries between GST grains, as soon as a Ge grain disappears, the GST grain boundary network is modified. The second way of reorganization is due to the coalescence of Ge grains and to the motion of grain boundaries which evolve so that their local curvature is reduced. Indeed, when two Ge grains coalesce nothing can hinder the grain boundary motion. Those two mechanisms can be seen in Fig. 2e and Fig. 2f.

V. Coupling with an electro-thermal solver

To simulate Joule heating during device operations, an electro-thermal solver is used; temperature fields obtained from the electro-thermal simulations are then used by the MPFM model. The electro-thermal solver relies on the coupled system of partial differential equations formed by the charge conservation and the heat transfer equations :

$$\nabla \cdot (-\sigma \nabla V) = 0 \tag{16}$$

$$\rho C_p \frac{\partial T}{\partial t} + \nabla \cdot (-k_{th} \nabla T) = \sigma (\nabla V)^2 \tag{17}$$

where σ, ρ, C_p and k_{th} stand for the materials electrical conductivity, density, heat capacity and thermal conductivity. Electrical and thermal conductivity of the Ge rich GST are modeled as function of temperature:

$$\sigma_{\text{pcm}} = \frac{\sigma_0}{2}\left(\tanh(B_e T + C_e) + D_e\right) \tag{18}$$

$$k_{th,pcm} = \frac{k^0_{th}}{2}\left(\tanh(B_{th} T + C_{th}) + D_{\text{th}}\right) \tag{19}$$

A set of parameters for electrical and thermal conductivity for Ge-rich GST was fixed (see Table I) in order to obtain current-voltage curves close to experimental results.

TABLE I: Parameters for Ge-rich GST electrical and thermal conductivity

σ_0	B_e	C_e	D_e
$2.8 \cdot 10^4 S/m$	$0.0022K^{-1}$	-1.8	1
k^0_{th}	B_{th}	C_{th}	D_{th}
$2.566W/K/m$	$0.0051K^{-1}$	-48.359	1.418

The system of electro-thermal equations is solved using the Finite Element method with COMSOL Multiphysics®. The MPFM equations are discretized using the Finite Difference method on a cartesian grid with an Euler explicit time discretization. The coupling between the electro-thermal model and the MPFM model has been implemented first with a simplified approach; the electro-thermal equations are solved without taking into account phase changes. At each time t^n, the electro-thermal equations are computed with a time step of

$10^{-9}s$. Then one nanosecond of the MPFM is computed using the value of temperature field at t^n. This is actually CPU-time expensive because of the explicit time scheme which implies a stability condition on the time step ($dt < 7.8\,10^{-13}s$).

VI. Simulation Results and Discussion

The device simulated is a state-of-the-art PCM device [1] comprising a wall storage element (Fig. 3a) to which a trapezoidal pulse of 6μs with a plateau of $100ns$ is applied. With a current of the order of the melting current, Joule heating is high enough, during the plateau of the trapezoidal pulse, for the melting of the active zone of the PCM material as illustrated by the temperature field (Fig. 3b and 3c). For this

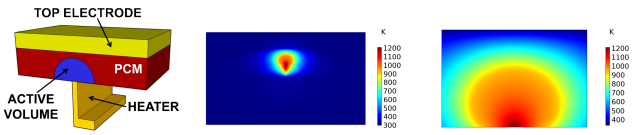

(a) Wall Structure (b) Tmax/Wall Structure (c) Tmax/Active PCM

Fig. 3: Joule heating simulation of the Wall Structure

simulation, the PCM layer is initially in a polycristalline state as obtained from a isothermal recrystallization (fig. 4a). As illustrated by Fig. 4c, the active domain of PCM is partially melted during the pulse. When the current is ramped down, the temperature decreases, and crystallization takes place with the coupled growth of the two crystalline phases: the Ge phase and the GST phase. The exchange of Ge atoms between the two phases is a determining factor of the crystallization kinetics. From 1.6μs the Ge phase is not growing any more (the grains of the Ge phase have the same shape in Fig. 4e and Fig. 4f). When the GST phase is the only one growing, the remaining melted domain gets richer in germanium and this leads to the nucleation of the Ge phase in the central domain (Fig. 4f). Among the main differences between the microstructures at the initial state (Fig. 4a) and at the end of the recrystallization (Fig. 4f), we see clearly a redistribution of germanium. Our simulation confirms qualitatively the impoverishment of germanium of the active domain and the accumulation of germanium on the periphery of this active domain that was already highlighted by experimental results [12].

VII. Conclusion and Perspectives

We have implemented a Multi-Phase Field Model to simulate the non congruent phase change of a Ge-rich GST alloy. This model takes into account the possibility of crystallization into two different phases, the stoichiometric GST225 and an almost pure Ge phase, and resolves the orientation of the crystal grains. We have used a simplified thermodynamic description in terms of a pseudobinary phase diagram, and we have adjusted the parameters of this diagram as well as the kinetic parameters of the model to experimental data available in the literature. This work brings a novel implementation of the Multi-Phase Field Model and its coupling to an electrothermal solver. As of now, the method is clearly only qualitative, and

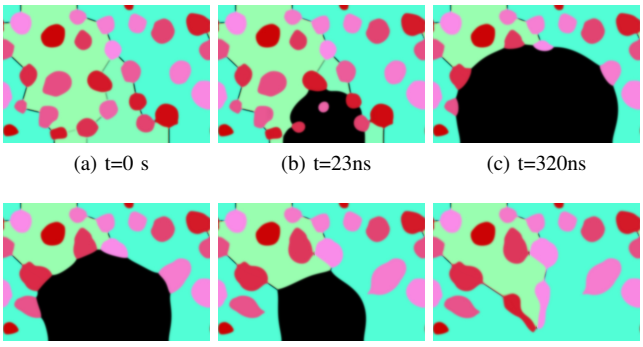

(a) t=0 s (b) t=23ns (c) t=320ns

(d) t=930ns (e) t=1.6μs (f) t=2.8μs

Fig. 4: Temporal evolution of the microstructures during the application of a trapezoidal current pulse to the Wall Structure with the PCM initially in polycrystalline state. The color code is the same as in Fig.2

numerical optimization is still needed to allow for intensive simulations, but our work already paves the way to a better understanding of the complex phenomena (including germanium segregation and grain boundary evolution) that take place during operations in GST-based PCM. This work was funded by the Association Nationale Recherche Technologie (ANRT), France, and STMicroelectronics through the CIFRE contract number 2016/1237.

References

[1] F. Arnaud et al, "Truly Innovative 28nm FDSOI Technology for Automotive Micro-Controller Applications embedding 16MB Phase Change Memory," IEDM Tech. Dig. Dec. 2018

[2] G. Navarro et al, "Trade-off Between SET and Data Retention Performances Thanks to Innovative Materials for Phase-Change Memory," IEDM Tech. Dig. Dec. 2013, pp. 21.5.1-21.5.4

[3] O. Cueto, V. Sousa, S.Blonkowski, G.Navarro, "Coupling the Phase-Field Method with an Electrothermal Solver to Simulate Phase Change Mechanisms in PCRAM Cells," proceedings of IEEE conf. SISPAD 2015

[4] H. Henry, J. Mellenthin, and M. Plapp, "Orientation-field model for polycrystalline solidification with a singular coupling between order and orientation," Phys. Rev. B **86**, 054117 (2012)

[5] R. Folch and M. Plapp, "Quantitative phase-field modeling of two-phase growth," Phys. Rev. E **72**, 011602 (2005)

[6] M. Plapp, "Unified derivation of phase-field models for alloy solidification from a grand-potential functional," Phys. Rev. E **84**, 031601 (2011)

[7] J. Orava, A. L. Greer, B. Gholipour, D. W. Hewak, C. E. and Smith, "Characterization of supercooled liquid Ge2Sb2Te5 and its crystallization by ultrafast-heating calorimetry," Nat. Mater. 2012, 11, 279–283 DOI: 10.1038/nmat3275

[8] S. Bordas, M.T Clavaguer-Mora, B. Legendre and C. Hancheng, "Phase diagram of the ternary system Ge-Sb-Te: II. The subternary Ge-GeTe-Sb2Te3-Sb," Thermochim. Acta, 107 (1986), pp. 239-265

[9] G. Novielli, A. Ghetti, E. Varesi, A. Mauri, R. Sacco, "Atomic migration in phase change materials," IEDM Tech. Dig. Dec. 2013

[10] C. Reina, L. Sandoval, J. Marian, "Mesoscale computational study of the nanocrystallization of amorphous Ge via a self-consistent atomistic phase-field model, ", Acta Mater. 77, 2017, 335-351

[11] M. Agati, M. Vallet, S.Joulié, D. Benoit and A. Claverie, "Chemical phase segregation during the crystallization of Ge-rich GeSbTe alloys,", Journal of Materials Chemistry C, 2019, 7,8720

[12] P. Zuliani et al, "Overcoming Temperature Limitations in Phase Change Memories With Optimized GeSbTe," IEEE Trans. Electronics Devices v60 n12, pp.4020, 2013